

**VANADIUM VALENCE AS A SENSOR OF OXYGEN FUGACITY IN BUFFERED EXPERIMENTS AT HIGH PRESSURE.** K. Richter<sup>1</sup>, K.M. Pando<sup>1</sup>, A.L. Butterworth<sup>2</sup>, C. E. Jilly-Rehak<sup>2</sup>, Z. Gainsforth<sup>2</sup>, D.K. Ross<sup>1</sup>, A.J. Westphal<sup>2</sup>; <sup>1</sup>Johnson Space Center, Houston, TX 77058; kevin.richter-1@nasa.gov. <sup>2</sup>Space Sciences Laboratory, University of California Berkeley, Berkeley, CA 94720.

**Introduction:** Oxygen fugacity is an intensive parameter that controls fundamental chemical and physical properties in planetary materials [1]. For example, in terrestrial magmas high  $fO_2$  promotes magnetite stability and low  $fO_2$  causes Fe-enrichment due to magnetite suppression. On the other hand, the low  $fO_2$  typical of lunar and asteroidal basalts allows metal to be stable. Experimental studies of magmatic systems will therefore be most useful if they are done at a specific and relevant  $fO_2$  for the samples under consideration. Control of  $fO_2$  in the solid media apparatus (piston cylinder or multi-anvil) has relied on either sliding sensors or graphite capsule buffering, which are of limited application to astromaterials that record a wide range of  $fO_2$ . Here we describe a new approach that allows  $fO_2$  to be specified across a wide range of values relevant to natural samples.

**Experimental approach:** The general approach is use of a double capsule design where the outer capsule is the metal of the buffer, and inside the bottom of the outer capsule is a layer of the oxide portion of the buffer. Metal-oxide pairs used for the outer buffer capsule were – in order of most oxidized to most reduced – Co-CoO, Mo-MoO<sub>2</sub>, W-WO<sub>3</sub>, Cr-Cr<sub>2</sub>O<sub>3</sub>, Ta-Ta<sub>2</sub>O<sub>5</sub>, and Nb-Nb<sub>2</sub>O<sub>5</sub>. The  $fO_2$  defined by these pairs was calculated using thermodynamic data, mainly from [2], as well as [3-5].

The inner capsule contains the sample of interest (Fig. 1), and can be MgO, alumina or graphite. Although the ultimate goal is to study natural systems – such as chondritic or primitive materials, metal-silicate or mineral-melt element partitioning, phase equilibria studies, or mineral or melt syntheses – the more specific goal of this study is to document the variation of  $fO_2$  within the inner capsule using a known  $fO_2$  sensor. For this, we utilized V-doped glasses in the CaO-MgO-Al<sub>2</sub>O<sub>3</sub>-SiO<sub>2</sub> system (diopside-anorthite eutectic melt in the CMAS system) in an alumina capsule. These V-doped glasses equilibrated at a range of  $fO_2$  buffers should exhibit variation in V K-edge XANES pre-edge peak intensity and energy, as calibrated by [6].

The samples were loaded into a 13 mm non-end-loaded piston cylinder apparatus, using a BaCO<sub>3</sub> pressure medium, a graphite furnace, and temperature monitored with a Type C thermocouple [6]. Samples were pressurized to 1 GPa, and heated to 1400 °C, and held for 3 hours before power quenching to room temperature. Run products were mounted in epoxy and sectioned for analysis by SEM, EMPA, and X-ray Absorption Near Edge Structure (XANES) spectroscopy.

**Analytical approach:** Run product textures and overall mineralogy was surveyed using a JEOL 7640 FEG-SEM, and metal-oxide and silicate phases were analyzed with a JEOL 8530 FE Hyperprobe. V in glasses was analyzed at the hard X-ray microprobe synchrotron beamline 10.3.2, situated at a bend magnet source at the Advanced Light Source (ALS), Lawrence Berkeley National Laboratory. The ALS operates at 1.9 GeV, 500 mA current, and beamline 10.3.2 provides up to 10<sup>9</sup> photons/s at 6 keV. We took 2  $\mu$ m spatial resolution X-ray fluorescence multi-element maps to select a single phase area, then acquired cumulative V K-edge XANES spectra from one spot (5 x 2  $\mu$ m). The spectra were deadtime corrected, energy-calibrated with a V metal foil standard, and normalized following the method in [6].

**Results:** Verification of the buffer was done by SEM and EMPA. The former was used to image the textures and the latter to confirm stoichiometry of the oxide phase. For example, the experiment with the Ta-Ta<sub>2</sub>O<sub>5</sub> buffer (Fig. 1a) had a ~100  $\mu$ m thick layers of Ta metal and Ta<sub>2</sub>O<sub>5</sub>. The use of a Mo outer capsule in some cases was to maintain capsule integrity while including the metal half of the buffer along with the oxide in the bottom of the outer Mo capsule.

The diopside-anorthite eutectic melt reacted in some cases with the alumina capsule to stabilize plagioclase feldspar (Fig. 1b). The silicate melts thus gained Al<sub>2</sub>O<sub>3</sub> from reaction, and also in most cases dissolved oxides of the buffer material such as CoO, WO<sub>3</sub>, Nb<sub>2</sub>O<sub>5</sub>, and MoO<sub>2</sub>. Although the glasses contain 0.35 to 0.40 wt% V<sub>2</sub>O<sub>3</sub>, the plagioclase contained V below detection limits, consistent with the incompatibility of V measured by [7].

V XANES spectra of the CMAS glasses exhibit pre-edge peaks associated with V<sup>3+</sup> [6,8]. Pre-edge peaks for the glasses in this study occur around 5467-5469 eV (Figs. 2a,b). These peaks can be used to determine V valence (V\*) and also  $fO_2$  [6,8]. Using the normalized pre-edge peak intensities (Fig. 2b), V\* and  $fO_2$  were calculated for each glass (Table 1). Calculated  $fO_2$  correlates with the  $fO_2$  calculated for each buffer, with the exception of the Co-CoO buffered sample which has a slightly lower V valence and  $fO_2$  than expected. This indicates that the buffers are indeed imposing a specific  $fO_2$  in the sample environment, and that this experimental design can be used to study a wide range of  $fO_2$  with use of the buffers employed here.

**Conclusions:** The double capsule and buffer approach used here can control the  $fO_2$  environment in the piston cylinder sample assembly. This approach may be used to study a broad range of mineral and melt equilibria across a wide  $fO_2$  range relevant to natural astro-materials.

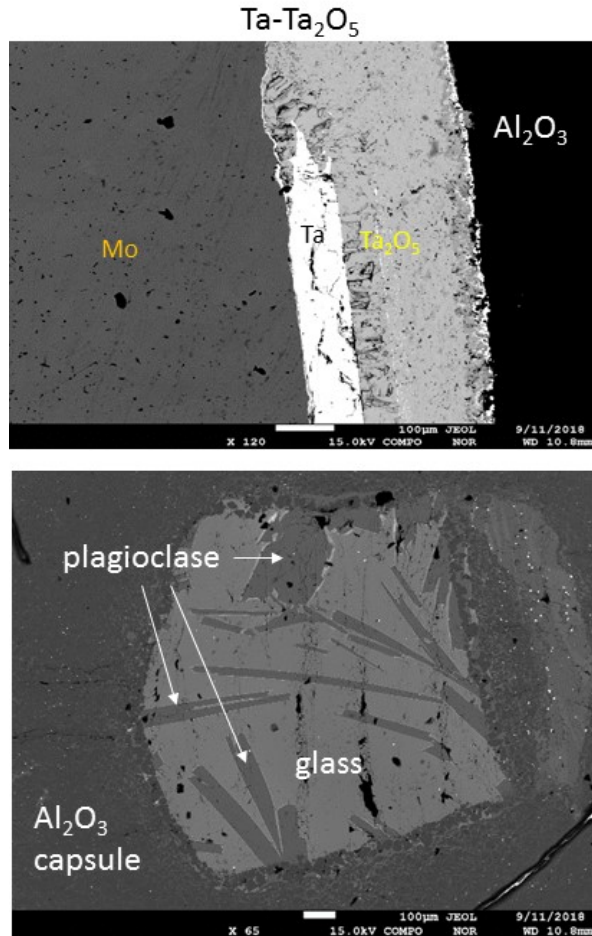


**Figure 1a (top):** BSE images of the buffer layer of Ta and  $Ta_2O_5$  at the bottom of the Mo outer capsule. **Figure 1b (bottom):** sample of CMAS composition that stabilized plagioclase feldspar and glass. The alumina capsule material encloses the CMAS composition.

**Table 1:** V XANES data for synthetic glasses.

Buffer	V XANES pre-edge peak intensity	V*	$fO_2$
Mo-MoO <sub>2</sub>	205	3.5	-8.95
Nb-Nb <sub>2</sub> O <sub>5</sub>	62	2.78	-12.62
Cr-Cr <sub>2</sub> O <sub>3</sub>	130	3.19	-10.35
Ta-Ta <sub>2</sub> O <sub>5</sub>	132	3.2	-10.30
W-WO <sub>3</sub>	198	3.47	-9.05
Co-CoO	198	3.47	-9.05

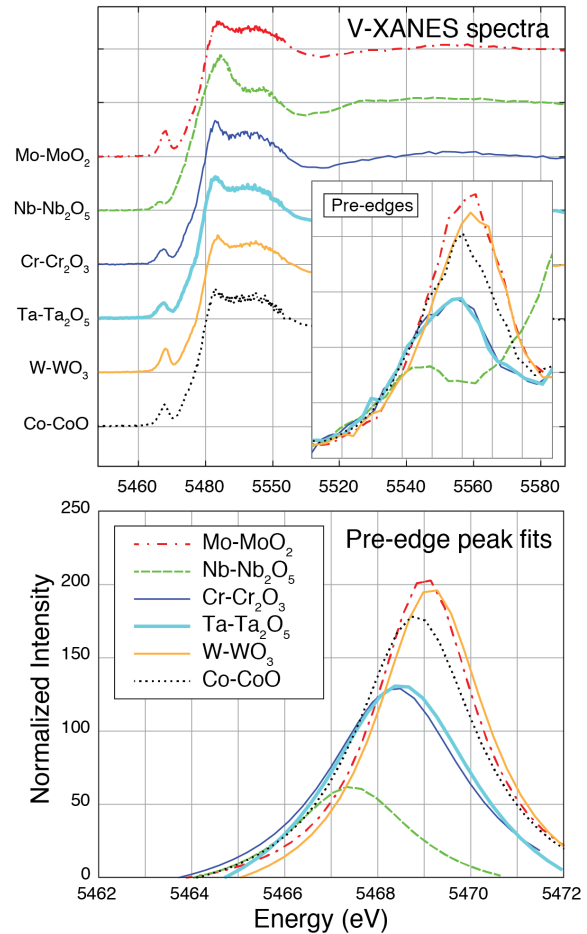


**Figure 2a (top):** Top: Stacked V XANES spectra for CMAS glasses equilibrated using outer capsule buffers Co-CoO, Mo-MoO<sub>2</sub>, W-WO<sub>3</sub>, Cr-Cr<sub>2</sub>O<sub>3</sub>, Ta-Ta<sub>2</sub>O<sub>5</sub>, and Nb-Nb<sub>2</sub>O<sub>5</sub>. Inset: Zoomed-in view of the pre-edge region of the V XANES spectra. Plot energy and intensity ranges are the same as in pre-edge peak fit plot below.

**Figure 2b (bottom):** Lorentzian peak fits for the normalized V XANES pre-edge spectra, after [6].

**References:** [1] Righter, K. et al. (2016) Amer. Min. 101, 1928-1942. [2] Barin, I. (1995) Thermochemical Data of Pure Substances, 3rd Ed., Wiley-VCH Verlag GmbH, Germany. [3] Raghavan, S. and Kay, D.A.R. (1990) Thermochim. Acta, 170, 13-17. [4] O'Neill H. St.C. and Pownceby, M. I. (1993) Contrib Mineral Petrol 114, 296-314. [5] Jacob, K.T. et al. (2010) J. Chem. Eng. Data 55, 4854-4863. [6] Sutton, S.R. et al. (2005) GCA 69, 2333-2348. [7] Bindemann, I. et al. (1998) GCA 62, 1175-1193. [8] Righter, K. et al. (2006) Amer. Min. 91, 1643-1656.

**Acknowledgements:** This research used resources of the Advanced Light Source, which is a DOE Office of Science User Facility under contract no. DE-AC02-05CH11231. We thank Sirine Fakra, beamline scientist at ALS 10.3.2.